The estimation problem and heterogenous swarms of autonomous agents

Guillaume Sartoretti[1], Max-Olivier Hongler[1], and Roger Filliger[2]

[1] Swiss Federal Institute of Technology in Lausanne
EPFL Campus, CH-1015 Lausanne, Switzerland
(e-mail: {guillaume.sartoretti,max.hongler}@epfl.ch)
[2] Bern University of Applied Sciences
Quellgasse 21, 2501 Biel/Bienne, Switzerland
(e-mail: roger.filliger@bfh.ch)

Abstract. We consider the situation of a homogeneous swarm of agents following a partially observable leader agent. The resulting, slightly heterogeneous swarm of agents is softly controlled by the leader. We study the swarm dynamics using a recently established connection existing between multi-agents dynamics and nonlinear optimal state estimation. For a whole class of nonlinear agents interactions, we are able to explicitly calculate the resulting swarm dynamics. We interpret the leader-follower dynamics as a nonlinear scalar feedback particle filtering problem which is closely related to the class of non-linear filters initially studied by V. E. Beneš. Despite its nonlinear character, the state estimation problem remains finite dimensional; it merely results from a change of measure in an underlying Ornstein-Uhlenbeck process. The agents interactions, which are driven by common observations of the randomly corrupted position of the leader, can be interpreted as the innovation kernel that underlies any Bayesian filtering issues. Numerical results fully corroborate our theoretical findings and intuition.
Keywords: Heterogeneous swarm, Multi-agent dynamics, Leader-based model, Nonlinear filtering, Feedback Particle Filter, Exact Results, Numerical Simulations.

1 Introduction

Among the vast and steadily increasing literature devoted to the dynamics of large number of mutually interacting autonomous agents, analytically solvable models able to stylize reality, or at least some aspect of it, are definitely welcome [1–4]. Despite features necessary for an analytical approach, these contributions strongly enhance our understanding of the emergence of collective phenomena like synchronization, aggregation, pattern formation, behavioral phase transitions, fashion and others. Most analytical studies focus on the dynamics of homogenous swarms of (identical) agents. Either the agents local rules are given and the ultimate goal is to analytically derive the emerging collective patterns or inversely, given a collective behavior, the goal is to unveil the agents local rules and their interactions. Purely homogeneous swarms are however rather uncommon.

In this paper, we focus our attention on slightly heterogeneous swarms in which one infiltrated agent (we call it the *leader*) is ultimately able to drive the whole swarm to adopt a desired objective [5]. Several types of leaders can be considered depending on the ways they interact with their fellows. Either the leader is external and hence is explicitly recognized by ordinary agents of the swarm [6,7], or it acts as a *shill* who purposely gives the impression to be independent while in fact obeying to a hidden master [8–10]. Besides very particular configurations [11,12], there is generally little hope for an analytical investigation of the collective behavior of a shill- or leader-infiltrated (and hence heterogeneous) swarm. It is the objective of this paper, to unveil a class of dynamical models for which this can be achieved.

Our source of inspiration for analytical models is taken from the realm of stochastic filtering. Roughly speaking, the evolution of a stochastically driven system $\mathcal{S}$ is monitored by an observer $\mathcal{O}$ which itself delivers noisy information. The filtering goal at time instant t is to construct a best possible estimation of the state $\mathcal{S}$ by processing information gained from $\mathcal{O}$ up to time t. The filtering process is achieved via *sequential Bayesian* steps. Specifically, one has a *prediction step* where one estimates the relevant conditional probability density function (pdf) based on the $\mathcal{S}$-dynamics and an *updating step* based on the $\mathcal{O}$-dynamics. For linear $\mathcal{S}$-evolutions driven by White Gaussian Noise (WGN) and simultaneously $\mathcal{O}$-measurements corrupted by WGN, the filtering problem is completely solvable and its solution is known as the *Kalman-Bucy filter*. Indeed, due to linearity and Gaussian noise, both the prediction and the updating steps conserve the Gaussian character of the relevant pdf's. Therefore the underlying filtering problem remains finitely dimensional as all operations

are expressible via means and covariances only. For nonlinear evolution, the Gaussian character is lost thus most likely leading to infinite dimensional problems. Analytical treatments are then precluded and in general only numerical approaches are feasible. In this context, particle filters methods and very recently *feedback particles algorithms* (FPA) are directly relevant for our present goal as they naturally allow to interpret particles as agents [13]. The FPA prediction step is achieved by attributing to an homogeneous swarm of agents the $\mathcal{S}$ dynamics. The updating processes, realized via mutual interactions of the agents with a mean field variable, will globally minimize, in real time, the Kullback-Leibler distance between the $\mathcal{S}$- and the observation updated probability density functions. In this paper, we view the $\mathcal{S}$-dynamics as playing the role of a leader evolving among an homogeneous swarm of N ordinary agents. When $N \to \infty$, this dynamics reduces to a *mean-field game*, [14,15] with infinitesimally short time horizon, (as real time updating – excluding smoothing – is realized). The FPA for stochastic filtering offers therefore a natural framework to construct leader driven swarms of agents. As a natural consequence, solvable filtering problems, like the Kalman-Bucy case, provide directly solvable heterogeneous swarms dynamics. Here, our intention is to construct a class of multi-agents models which simultaneously keep the associated FPA finitely dimensional and yet escape from the pure Gaussian world. The idea on which we base our construction, is to consider a class of "Girsanov-changes" of probability measures applied on Ornstein-Uhlenbeck dynamics (i.e. linear dynamics with Gaussian noise sources). The classical change of measure operation which is detailed in many places (see [16–18] for related applications) conserves the finite dimensional character of the filtering problem and provides another access to results obtained in [19,20].
We organize the paper as follows: in section 2, the explicit connection between the filtering problem and the driving of a swarm of agents infiltrated by a leader will be precised. In section 3, we introduce a specific example of swarms of non-Gaussian agents which are softly controlled by a leader and for which the associated FPA is analytically solvable. Section 4 is devoted to numerical experiments to comfort our analytical findings.

2 Multi-agent dynamics

Consider a swarm of N Brownian agents $\mathcal{A}_i$, $i = 1, 2, \cdots, N$, and one additional leader agent $\mathcal{A}$ with dynamics:

$$\begin{cases} dX_i(t) = f\left(X_i(t)\right)dt + \mathcal{K}\left(X_i(t), \boldsymbol{X}(t), dZ(t)\right) + \sigma dW_i(t), \\[2ex] \text{leader dynamics} \begin{cases} dY(t) = f\left(Y(t)\right)dt + \sigma dW(t), \\[2ex] dZ(t) = h\,Y(t)dt + \sigma_o dW_y(t), \end{cases} \end{cases} \tag{1}$$

where $h > 0$ is a constant, $f : \mathbb{R} \to \mathbb{R}$ is a function, $dW_i(t)$, $dW(t)$ and $dW_y(t)$ are mutually independent WGN processes and the vector $\boldsymbol{X}(t) = (X_1(t), X_2(t), \cdots, X_N(t))$ describes the dynamic state of the N homogenous agents. The *leader* agent $Y(t)$ affects the dynamics of the $X_i(t)$ via the interaction kernel $\mathcal{K}\left(X_i(t), \boldsymbol{X}(t), dZ(t)\right)$. We emphasize that the leader's dynamics $Y(t)$ itself is not affected by the behavior of the swarm $\boldsymbol{X}(t)$. The leader can be thought of as hiding its real position $Y(t)$ from its fellows agents, only allowing them access to the noisy value $Z(t)$ (the unveiled position). Agent $\mathcal{A}_i$ – trying to follow the noisy impression of the leaders position displacement $dZ(t)$ – will, in order to make a meaningful next step towards the most likely position of the leader, also take into account the displacements of all other agents (which in turn try also to undertake the best step towards the most likely position of the leader). To achieve this, let us now specifically consider an interaction kernel of the form:

$$\mathcal{K}\left[X_i(t), \boldsymbol{X}(t), dZ(t)\right] = \nu\left(X_i(t), t\right) \otimes \left\{ dZ(t) - \underbrace{\frac{h}{2}\left[X_i(t) + \frac{1}{N}\sum_{k=1}^{N} X_k(t)\right]dt}_{\mathcal{G}[X_i(t), \boldsymbol{X}(t)]} \right\}, \tag{2}$$

where the coupling strength $\nu(X_i(t), t)$ is a positive convex function in $X_i(t)$ and where, due to the presence of multiplicative WGN processes, we define $\otimes$ to denote the Stratonovich interpretation of the underlying stochastic integrals. In Eq.(2), $\mathcal{G}\left[X_i(t), \boldsymbol{X}(t)\right]$ is a consensual position given by the average between agent $\mathcal{A}_i$'s position and the whole swarm barycenter. The interaction kernel compares the position increment $\mathcal{G}dt$ with the leader's unveiled position increment $dZ(t)$ and weights this stimulus with the coupling strength ν. The assumptions on ν imply that $\mathcal{K}\left[X_i(t), \boldsymbol{X}(t), dZ(t)\right]$ tends, in real time, to steadily reduce the distance between $\mathcal{G}\left[X_i(t), \boldsymbol{X}(t)\right] dt$ and $dZ(t)$. While the multiplicative factor $\nu(X_i(t), t)$ in Eq.(2) remains yet undetermined, its complete specification can be fixed by introducing a cost structure. In general, one could require that for some running cost functional $\mathcal{J}\left[\mathcal{K}, X_i(t), \boldsymbol{X}(t), \mathcal{Z}(t), t\right]$ and final cost $\Psi\left(X_i(T), \boldsymbol{X}(T), dZ(T)\right)$ at time horizon T, the interaction $\mathcal{K}$ is a minimizer of the associated optimization problem. More formally, the interaction kernel (and hence ν) would be the unique minimizer over a set $\mathbb{K}$ of admissible controls, namely:

$$\begin{aligned}
&\mathcal{K}\left[X_i(t), \boldsymbol{X}(t), dZ(t)\right] \\
&= \min_{K\in\mathbb{K}} \left\{ \left(\int_t^T \mathcal{J}\left[K, X_i(s), \boldsymbol{X}(s), dZ(s), s\right] ds \right) + \Psi\left(X_i(T), \boldsymbol{X}(T), dZ(T)\right) \right\}.
\end{aligned} \tag{3}$$

The coupled set of Eqs.(1) and (3) can be interpreted as a multi-players differential game [21]. For large populations one can use the empirical density $P^{(N)}(x,t)$ to approximate the mean field posterior density $P(x,t \mid \mathcal{Z}(t), x_0)$:

$$P^{(N)}(x,t)dx = \frac{1}{N}\sum_{n=1}^{N} \mathbf{1}\left\{X_n(t) \in [x, x+dx]\right\} \approx P(x,t \mid \mathcal{Z}(t), x_0)dx, \tag{4}$$

where the condition $\mathcal{Z}(t)$ is the information history of the process Z until time t and x_0 the initial location of the agents. In the $N \to \infty$ limit, we have:

$$\lim_{N\to\infty} \frac{1}{N}\sum_{k=1}^{N} X_k(t) = \int_{\mathbb{R}} x' P(x', t \mid \mathcal{Z}(t), x_0)dx' = \mathbb{E}\left\{X(t) \mid \mathcal{Z}(t)\right\} \tag{5}$$

where $X(t)$ is the mean field variable associated to the mean field posterior density $P(x,t \mid \mathcal{Z}(t), x_0)$. The Fokker-Planck equation which governs this mean field posterior density reads (with a slight but self explaining abuse of notation for $\mathcal{K}$):

$$\tfrac{\partial}{\partial t} P(x,t \mid \mathcal{Z}(t), x_0) = -\tfrac{\partial}{\partial x}\left\{\left[a(x) + \mathcal{K}\left(x, \mathbb{E}\left\{X(t) \mid \mathcal{Z}(t)\right\}\right)\right] P(x,t \mid \mathcal{Z}(t), x_0)\right\} + \tfrac{\sigma^2}{2}\tfrac{\partial^2}{\partial x^2} P(x,t \mid \mathcal{Z}(t), x_0). \tag{6}$$

Note that Eqs.(6) and (3) define in a forward/backward coupling a so called differential *mean-field game problem.*

Feedback particles filters. For vanishing time horizon $T = t$ in Eq.(3), a simpler situation arises (the backward-coupling gets trivial) and the minimization is reduced to solving an Euler-Lagrange variational problem (ELP) for $\Psi\left(x, \mathbb{E}\left\{X(t) \mid \mathcal{Z}(t)\right\}\right)$. Choosing the objective criterion Ψ to be the Kullback-Leibler distance d_K:

$$\begin{cases}
\Psi\left(x, \mathbb{E}\left\{X(t)\right\}, dZ(t)\right) := d_K\left\{P(x', t \mid \mathcal{Z}(t), x_0); Q(x,t \mid x_0)\right\}, \\[2ex]
d_K\left\{P(x', t \mid \mathcal{Z}(t), x_0); Q(x,t \mid x_0)\right\} := \int_{\mathbb{R}} P(x', t \mid \mathcal{Z}(t), x_0)\left\{\ln\left[\frac{P(x',t\mid\mathcal{Z}(t),x_0)}{Q(x',t\mid x_0)}\right]\right\} dx',
\end{cases} \tag{7}$$

with $Q(x,t \mid x_0)$ being the transition probability density of the diffusion process $Y(t)$ defined in Eq.(1) we find the ELP:

$$\begin{cases}
-\frac{\partial}{\partial x}\left\{\frac{1}{P(x,t\mid\mathcal{Z}(t),x_0)}\frac{\partial}{\partial x}\left[P(x,t \mid \mathcal{Z}(t), x_0)\nu(x,t)\right]\right\} = \frac{h}{\sigma^2}, \\[2ex]
\lim_{|x|\to\infty} P(x,t \mid \mathcal{Z}(t), x_0)\nu(x,t) = 0,
\end{cases} \tag{8}$$

which leads to:

$$\begin{cases}
\nu(x,t) = \frac{h}{\sigma^2 P(x,t\mid\mathcal{Z}(t),x_0)}\left\{\int_{-\infty}^{x}\left[\mathbb{E}\left\{X(t) \mid \mathcal{Z}(t)\right\} - x'\right] P(x',t \mid \mathcal{Z}(t), x_0)dx'\right\}, \\[2ex]
\mathbb{E}\left\{X(t) \mid \mathcal{Z}(t)\right\} = \int_{-\infty}^{+\infty} x' P(x', t \mid \mathcal{Z}(t), x_0)dx'.
\end{cases} \tag{9}$$

Eqs.(1), (2) together with $\nu(x,t)$ given in Eq.(9) produce a nonlinear continuous time feedback particle filter. This realizes a direct reinterpretation of the leader-based dynamics in terms of a stochastic filtering problem. An example is detailed in the next section.
It is worthwhile noting that the leader influences the swarm through the variance σ (and the parameter h), and not only through its position. As σ grows, the agents uncertainties on the actual leader position increase. Consequently the coupling strength $\nu(x,t)$ decreases, the agents variances increase and the swarm will form a very widespread group of agents around the leader. Alternatively, small values for σ will allow for very compact swarm formation.

3 Finite dimensional filtering with Weber parabolic functions

Let us now introduce a specific filtering problem which will be related to the soft control of the multi-agents dynamics. The nonlinear filtering problem is to estimate the value of the one-dimensional state $Y(t)$, at time t, given a set of measurements prior to t: $\mathcal{Z}(t) = \{Z(s) \mid 0 \leq s \leq t\}$. We will treat hereafter time-continuous measurements and assume that the leader state $Y(t)$ – starting at position y_0 – evolves in time according to the stochastic differential equation:

$$\begin{aligned} dY(t) &= \overbrace{\left\{ \frac{d}{dy} \left[\log \mathcal{Y}_B(y)\right] \Big|_{y=Y(t)} \right\}}^{:=f_B[Y(t)]} dt + dW(t), \\ Y(0) &= y_0 \end{aligned} \tag{10}$$

in which W is standard Brownian motion and where $\mathcal{Y}_B(y)$ is the Weber parabolic function, solution to the ordinary differential equation

$$\frac{d^2}{dy^2}\mathcal{Y}_B(y) = \left[\frac{y^2}{4} + \left(B - \frac{1}{2}\right)\right]\mathcal{Y}_B(y) \tag{11}$$

with B being a control parameter. From the definition of $f_B[Y(t)]$, we easily see that

$$\frac{d}{dy}f_B(y) + f_B^2(y) = \frac{\frac{d^2}{dy^2}\mathcal{Y}_B(y)}{\mathcal{Y}_B(y)} = \frac{y^2}{4} + \left(B - \frac{1}{2}\right), \tag{12}$$

thus leading to a Beneš type filtering problem (a fully analytical approach to filtering problems in the Beneš class can be found in [20]) which can be solved optimally using only a finite number of statistics. In the sequel, we shall impose the parameter range $B \in \mathbb{R}^+$ which ensures the positivity of $\mathcal{Y}_B(y)$ ($\forall\, y \in \mathbb{R}$). For $B \in [0, 1/2]$, we further observe that the potential $-\log[\mathcal{Y}_B(y)]$ is locally attractive near the origin and asymptotically repulsive for $|y| \to \infty$. In the parameter range $B > 1/2$, the potential is systematically repulsive $\forall y \in \mathbb{R}$. Figure 1 shows the shape of $\mathcal{Y}_B(y)$ and $f_B(y)$ for different values of the control parameter B.
We observe the appealing possibility to obtain the couple of linear limiting cases:

$$\begin{cases} \mathcal{Y}_0(y) = e^{-\frac{1}{4}y^2} \quad \Rightarrow \quad f_0(y) = -\frac{1}{2}y \\ \\ \mathcal{Y}_1(y) = e^{+\frac{1}{4}y^2} \quad \Rightarrow \quad f_1(y) = +\frac{1}{2}y \end{cases} \tag{13}$$

and note that these linear cases are stable for $B = 0$ and unstable for $B = 1$. We now suppose that the linear measurement process $Z(t) \in \mathbb{R}$ (the *leader*'s unveiled position) from Eq.(1) follows the dynamic

$$dZ(t) = hY(t)dt + \sigma dW_1(t), \tag{14}$$

with $W_1(t)$ a standard Brownian motion independent of W and y_0, $h > 0$ a known scalar quantity and $\sigma > 0$ a constant diffusion coefficient.
Using the framework introduced in [20], the continuous time filter is given by the normalized probability density $P(y, t|\mathcal{Z}_t)$ of observing $Y(t) := y$ conditioned on the set of measurements up to time t, $\mathcal{Z}(t)$, and can be written in the form (computational details are given in the Appendix):

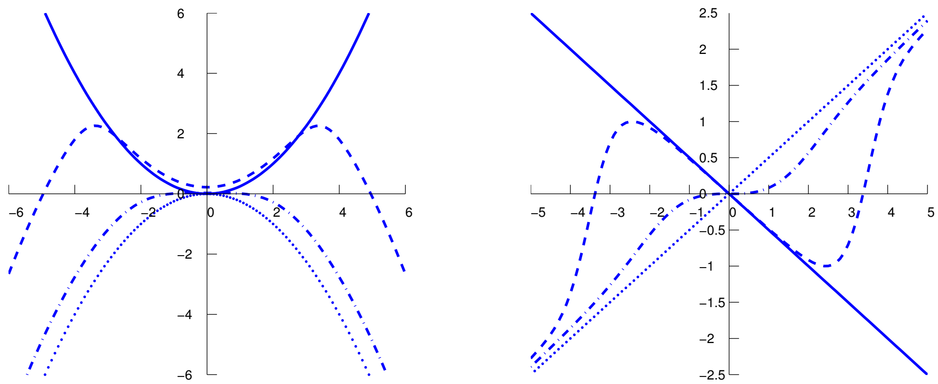

Fig. 1. Shape of $\mathcal{Y}_B(y)$ (left) and $f_B(y)$ (right) for $B = 0$ (plain line), $B = 0.01$ (stripped line), $B = 0.5$ (stripped-dotted line) and $B = 1$ (dotted line). For $B = 0$ the filtering problem is linear and the dynamics stable. For $B = 1$ the filtering problem is again linear but with unstable dynamics. In between, we have a non-linear filtering problem and the conditional probability density changes – with increasing B – from unimodal to bimodal and back to unimodal.

$$P(y,t) := P(y,t \mid \mathcal{Z}(t)) = \frac{\mathcal{Y}_B(y) \cdot e^{-\frac{(y-m)^2}{2s}}}{\mathcal{J}_0(m,s,B)} \tag{15}$$

with $\mathcal{J}_0(m,s,B)$ the normalization function:

$$\mathcal{J}_0(m,s,B) = 2\sqrt{\frac{\pi s}{2+s}} \left[\sqrt{\frac{2+s}{2-s}}\right]^B e^{\frac{m^2 s}{2(4-s^2)}} \mathcal{Y}_B\left(\frac{2m}{\sqrt{4-s^2}}\right). \tag{16}$$

The measurement *dependent* quantities $m := m(Z(t);t)$ are given by

$$m = m(Z(t);t) = \frac{\tanh(pt)}{p}\left[h\int_0^t \frac{\sinh(ps)}{\sinh(pt)} dZ(s) + \frac{py_0}{\sinh(pt)}\right] \tag{17}$$

and similarly, the measurement *independent* quantities $s := s(t)$ read as:

$$s = s(t) = \frac{1}{p}\tanh(pt) \tag{18}$$

with the definition $p = \sqrt{h^2 + \frac{1}{4}}$. With this expression for $P(y,t)$, we have for the conditional mean:

$$\langle Y_t \rangle := \mathbb{E}(Y_t|\mathcal{Z}(t)) = \frac{4m}{4-s^2} + \frac{2s}{\sqrt{4-s^2}} f_B\left[\frac{2m}{\sqrt{4-s^2}}\right] \tag{19}$$

and after lengthy but elementary manipulations the conditional variance:

$$var(Y_t) := \mathbb{E}((Y_t - \langle Y_t\rangle)^2|\mathcal{Z}(t)) = \frac{2s}{2+s} + \frac{4s^2}{4-s^2}\left\{\frac{m^2}{4-s^2} + B - f_B^2\left(\frac{2m}{\sqrt{4-s^2}}\right)\right\}. \tag{20}$$

Remark: For the couple of linear cases $B = 0$ and $B = 1$ from Eq.(13), we consistently find the following classical results:

$$P(y,t) = \frac{\left\{-\frac{((2+s)y-2m)^2}{4s(2+s)}\right\}}{\sqrt{2\pi\frac{2s}{2+s}}}, \qquad \langle Y_t\rangle = \frac{2}{2+s}m, \qquad var(Y_t) = \frac{2}{2+s}s \tag{21}$$

for $B = 0$ and

$$P(y,t) = \frac{\left\{-\frac{((2-s)y-2m)^2}{4s(2-s)}\right\}}{\sqrt{2\pi\frac{2s}{2-s}}}, \qquad \langle Y_t\rangle = \frac{2}{2-s}m, \qquad var(Y_t) = \frac{2}{2-s}s \tag{22}$$

for $B = 1$. Moreover, the coupling strength $\nu(x,t)$ reduces – as predicted by the linear version of the feedback filter – in both cases $B = 0$ and $B = 1$ to the standard, state independent Kalman gain:

$$\nu(x,t) = \nu(t) = \frac{h}{\sigma^2} var(Y_t). \tag{23}$$

4 Numerical results

Numerical results are obtained by simulating (1) for a finite swarm with $N < \infty$ agents and one leader. Thanks to the consistency of the estimator (see [13]), one can still use the results from the mean field analysis for large enough N. In this case $P(y,t)$ must be fitted against the empirical histogram of agents' position at time t, to find the values for m and s. The control $\nu(x,t)$ can then be numerically computed from its integral expression Eq.(9), while $\langle Y \rangle_t$ can be computed from Eqs.(19). The quantity $\frac{d}{dx}\nu(x,t)$ is computed by noting the relation $\frac{\frac{d}{dx}P(x,t)}{P(x,t)} = f_B(x) + \frac{x-m}{s}$, which can be written as:

$$\frac{d}{dx}\nu(x,t) = \frac{h}{\sigma^2}\left(\langle Y \rangle_t - x\right) - \nu(x,t) \cdot \left(f_B(x) - \frac{x-m}{s}\right). \tag{24}$$

Note that this straightforward fitting strategy to estimate $P(y,t)$ is – computationally – very costly. Extensive numerical computations have shown that $\nu(x,t)$ can safely be computed from Eq.(9) when using directly the empirical histogram of the agents' position instead of the fitted function in (15). $\frac{d}{dx}\nu(x,t)$ can then be numerically computed as $\frac{\nu(x+h,t)-\nu(x,t)}{h}$, by selecting a reasonably small value h.

Numerical results in linear cases. Figures 2 and 3 show in red the time evolution of the noisy leader's unveiled position. Standard Kalman-Bucy filtering techniques – with perfect knowledge on the initial condition and discrete time-step $dt = 2 \cdot 10^{-3}$ – will deliver the green line; which is the best estimate (i.e., minimizing the error covariance) for the leader's position. The mean value from the swarm of agents (likewise the output of the feedback particle filter) produces the much smoother blue curve. Both filtering methods can be quantitatively seen to produce the same average error through time (underlying the excellent accuracy performance of the agents based estimator).

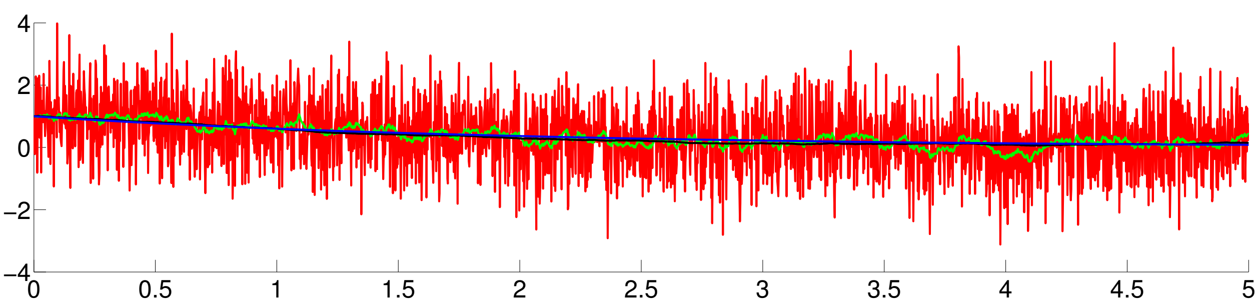

Fig. 2. Leader's position $Y(t)$ from Eq.(10) (black), along with its unveiled position $\mathcal{Z}(t)$ (red), for $B = 0$, $\sigma = h = 1$ and $t \in [0;5]$. In green, the output of the linear Kalman approach, and in blue the mean value $\langle Y \rangle_t$ measured from a swarm of $N = 1000$ agents. The particles start with $Y_i(0) = x_0 = 1\ \forall i$, while $Z(0) = Y(0) = x_0$.

Numerical results in nonlinear cases. We now concentrate on the parameter range $0 < B < 0.5$ as for $B \geq 0.5$ the swarms dynamics is similar to a repulsive- and for $B = 0$ equivalent to an attractive Ornstein-Uhlenbeck process (see Figure 1). For $0 < B < 0.5$ the dynamics of the leader is non-linear and shows an attractive potential in the central region (i.e., around the origin), and a repulsive potential for $|x| \gg 0$. Between these two regions the potential changes from attractive to repulsive and the leader undergoes strong nonlinear dynamics. Note that the attractive region is meta-stable and a leader starting within this region will finally escape.

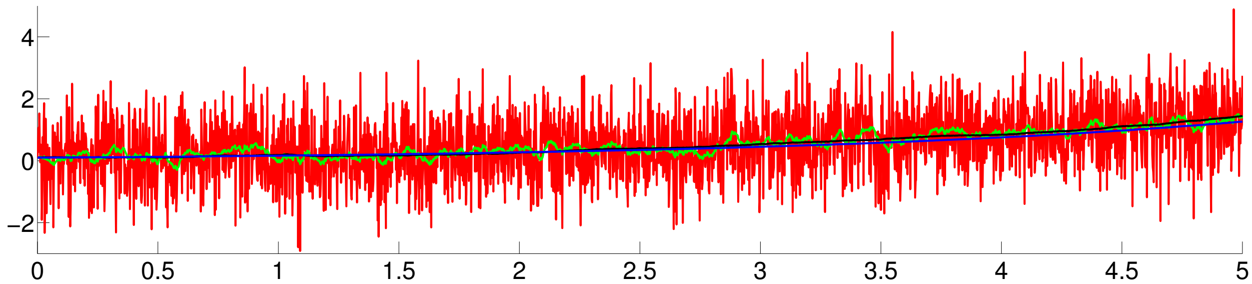

Fig. 3. Leader's position $Y(t)$ from Eq.(10) (black), along with its unveiled position $\mathcal{Z}(t)$ (red), for $B = 1$, $\sigma = h = 1$ and $t \in [0; 5]$. In green, the output of the linear Kalman approach, and in blue the value $\langle Y \rangle_t$ measured from a swarm of $N = 1000$ agents. The particles start with $Y_i(0) = x_0 = 0.1\ \forall i$, while $Z(0) = Y(0) = x_0$.

During the sojourn time of the leader in the attractive region, the close by agents undergo quasi linear dynamics. They too will remain in this attractive region, arrange in the vicinity of the leader's position and empirically realize the a posteriori distribution $P(y, t)$. As soon as the leader escapes from the attractive region, the other agents will start feeling the effect of their barycentric control kernel and ultimately follow the leader outside the meta-stable region. For an infinite swarm of agents, the conditional barycenter of the swarm will follow the leader's position with nearly no delay; but in our case with $N < \infty$ agents, a delay will be seen between the exit times of the leader and the agents. Figure 4 shows the result of a representative numerical simulation for $N = 1000$ agents, with a very narrow and shallow attractive region for $B = 0.49$.

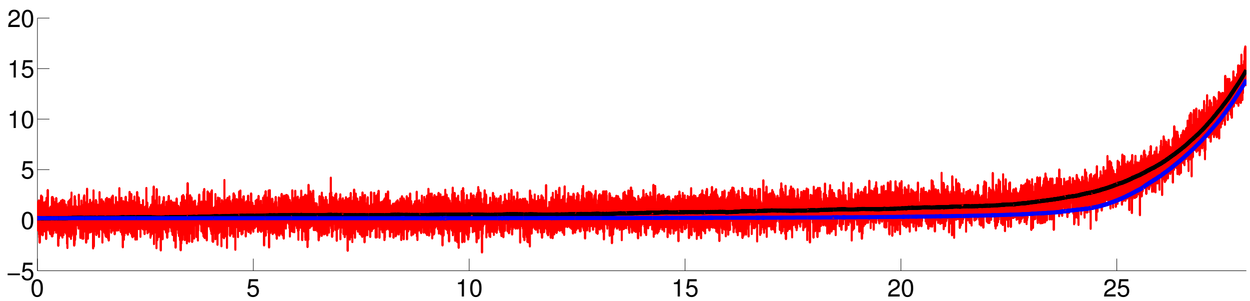

Fig. 4. Leader's position $Y(t)$ from Eq.(10) (black), along with its unveiled position $\mathcal{Z}(t)$ (red), for $B = 0.49$, $\sigma = h = 1$ and $t \in [0; 30]$. In blue the value $\langle Y \rangle_t$ measured from a swarm of $N = 1000$ agents. The particles start with $Y_i(0) = x_0 = 0.2\ \forall i$, while $Z(0) = Y(0) = x_0$.

If we zoom into the region where the leader exits the attractive domain, we see how its action affects the rest of the swarm. Indeed, as the leader goes away from the swarm, the control $\nu(x, t)$ will grow larger and drive agents away from the attractive region. This process takes some time, and enhances the variance of the swarm. This can be seen in Figure 5, where we zoom on the period in which the leader and the agents escape from the attractive region in Figure 4. After the agents have successfully escaped from the attractive region, the variance of the swarm decreases again, as the agents more closely match the leader's position.
To illustrate the last remark of Sect. 2, Figure 6 shows the influence of the choice of σ on the delay between the exit times of the leader and the barycenter of the swarm. Note that the empirical barycenter of the swarm is always contained "within" the measures, meaning that the barycenter of the swarms always gives a better filtered value than the position $dZ(t)$ unveiled by the leader.

5 Conclusion

Heterogeneous multi agent systems are notoriously difficult to describe analytically. As proposed in this article, the simple idea of adding a "linearly" hidden leader agent, already offers the possibility to influence the swarm in many ways. The leader can for example softly control the spreading factor of the agents around

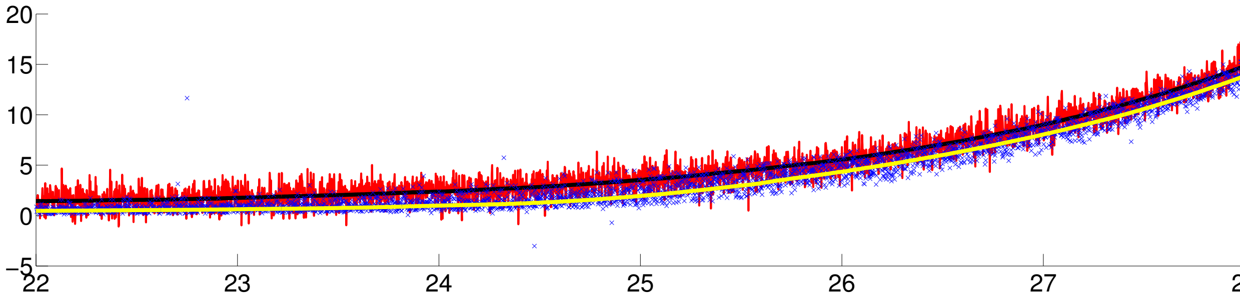

Fig. 5. Leader's position $Y(t)$ from Eq.(10) (black), along with its unveiled position $\mathcal{Z}(t)$ (red), for $B = 0.49$, $\sigma = h = 1$ and $t \in [0; 30]$. In yellow the value $\langle Y \rangle_t$ measured from a swarm of $N = 1000$ agents, and in blue the position of random agents (to visually show the variance of the swarm) through time. The particles start with $Y_i(0) = x_0 = 0.2\ \forall i$, while $Z(0) = Y(0) = x_0$.

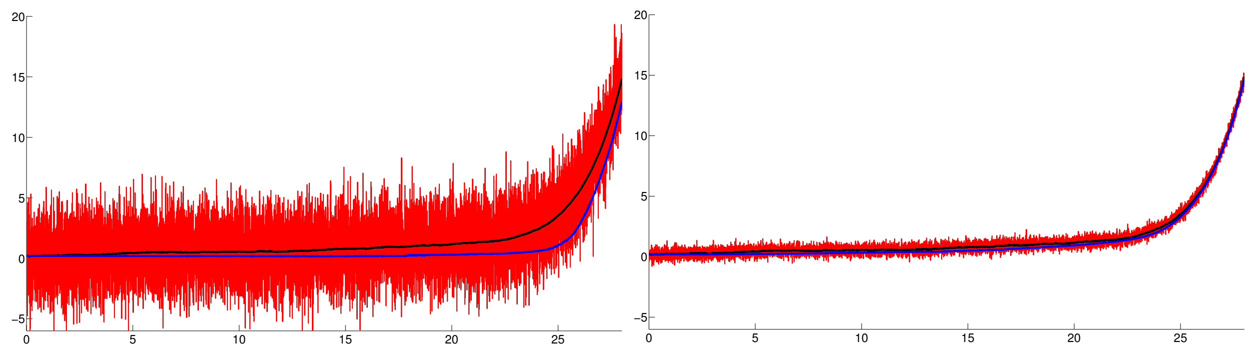

Fig. 6. Leader's position $Y(t)$ from Eq.(10) (black), along with its unveiled position $\mathcal{Z}(t)$ (red), for $B = 0.49$, $h = 1$, $t \in [0; 30]$ and $\sigma = 0.3, 2$ (left, right). In blue the value $\langle Y \rangle_t$ measured from a swarm of $N = 1000$ agents. The particles start with $Y_i(0) = x_0 = 0.2\ \forall i$, while $Z(0) = Y(0) = x_0$.

its position, by tuning its hiding parameter σ. This leader-based dynamic also exhibits the property that all agents know which of their fellow is the leader, but an external observer cannot discover this information from the observation of the swarm's behavior. The leader is seen from the outside as one of the regular agents, but effectively pilots the swarm from the inside.
Inspired from current techniques in optimal state estimation, analytical insight is made possible by restricting the agents dynamics to the Beneš class of finite dimensional filtering problems and to construct agents interaction kernels amenable, in the mean field approximation, to the classical innovations kernels of sequential optimal filtering. In future work we will explore the potentialities of mean field games where the interaction kernels result from an optimization procedure with finite time horizon T. It is prospected that analytical insight is still possible if the kernels are amenable to innovation kernels of sequential optimal *smoothing* problems.

References

1. M.-O. Hongler, R. Filliger, and O. Gallay. Local versus nonlocal barycentric interactions in 1d agent dynamics. *Mathematical Biosciences and Engineering*, 11(2):303–315, 2014.
2. R. Eftimie. Hyperbolic and kinetic models for self-organized biological aggregations and movement: A brief review. *Journal of mathematical biology*, 65(1):35–75, 2012.
3. N. Bellomo and C. Dogbe. On the modeling of traffic and crowds: A survey of models, speculations, and perspectives. *SIAM Review*, 53(3):409–463, 2011.
4. E. Bertin, M. Droz, and G. GrÃ©goire. Boltzmann and hydrodynamic description for self-propelled particles. *Physical Review E - Statistical, Nonlinear, and Soft Matter Physics*, 74(2), 2006.
5. J. Han Wang X. and H. Han. Special agents can promote cooperation in the population. *PLoS ONE 12, vol. 6*, 2011.

6. I. D. Couzin, J. Krause, N. R. Franks, and S. A. Levin. Effective leadership and decision-making in animal groups on the move. *Nature*, 433(7025):513–516, 2005.
7. M. Aureli and M. Porfiri. Coordination of self-propelled particles through external leadership. *EPL*, 92(4), 2010.
8. Dyer J. R. G. Faria J. J. and J. Krause. A novel method for investigating the collective behaviour of fish: Introducing 'robofish'. *Behavioral Ecology and Sociobiology 8, vol. 64, 1211-1218*, 2010.
9. Gribovskiy A., Halloy J., Deneubourg J.-L., H. Bleuler, and F. Mondada. Towards mixed societies of chickens and robots. *IEEE/RSJ 2010 International Conference on Intelligent Robots and Systems, Conference Proceedings pp. 4722-4728*, 2010.
10. L. Wang and L. Guo. Robust consensus and soft control of multi-agent systems with noises. *Journal of Systems Science and Complexity 3, vol. 21, 406-415*, 2008.
11. G. Sartoretti and Hongler M.-O. Soft control of swarms - analytical approach. In *Proceedings - International Conference on Agents and Artificial Intelligence 2013*, 2013.
12. G. Sartoretti and M.-O. Hongler. *Soft control of self-organized locally interacting brownian planar agents*, volume 8111 LNCS, PART 1 of *Lecture Notes in Computer Science (including subseries Lecture Notes in Artificial Intelligence and Lecture Notes in Bioinformatics)*. Springer, 2013.
13. T. Yang, P. G. Mehta, and S. P. Meyn. Feedback particle filter. *IEEE Transactions on Automatic Control*, 58(10):2465–2480, 2013.
14. S. Pequitoy, A.P. Aguiary, B. Sinopoli, and D.A. Gomes. Nonlinear estimation using mean field games. *NETG-COOP: International conference on NETwork Games, COntrol and OPtimization*, pages 1–10, 2011.
15. O. Guéant, J.-M.. Lasry, and P.-L. Lions. *Mean field games and applications*, volume 2003 of *Lecture Notes in Mathematics*. 2011.
16. J. C. Taylor. The minimal eigenfunctions characterize the ornstein-uhlenbeck process. *The Annals of Probability*, 17(3):1055–1062, 1989.
17. M.-O. Hongler. Study of a class of nonlinear stochastic process - boomerang behavior of the mean. *Physica D*, 2:353–369, 1981.
18. P. Dai Pra. Stochastic control approach to reciprocal diffusion processes. *Applied Mathematics and Optimization*, 23(3):313–329, 1991.
19. V. E. Beneš. Exact finite dimensional filters for certain diffusion with nonlinear drifts. *Stochastics*, 5:65–92, 1981.
20. F. E. Daum. Exact finite-dimensional nonlinear filters. *IEEE Transactions on Automatic Control*, AC-31(7):616–622, 1986.
21. A. Bensoussan, J. Frehse, and P. Yam. *Mean Field Games and Mean Field Type Control Theory*. Springer, 2013.
22. I. S. Gradshteyn and I. M. Ryzhik. *Table of integrals series and products*. Academic Press, 1980.

Appendix - Details of calculations

For the readers ease we introduce notations and collect formulae useful for the computation of the conditional probability density.

5.1 Collection of useful formulae

$$\sinh(x+y) = \sinh(x)\cosh(y) + \cosh(x)\sinh(y),$$

$$\cosh(x+y) = \cosh(x)\cosh(y) + \sinh(x)\sinh(y).$$

$$\int_{\mathbb{R}} e^{-ax^2-2bx-c}dx = \sqrt{\frac{\pi}{a}}e^{\frac{b^2-ac}{a}}, \qquad a>0$$

$$\int_{\mathbb{R}} \cosh[x\alpha]e^{-\frac{(x-\mu)^2}{\gamma}}dx = \sqrt{\pi\gamma}\cosh[\mu\alpha]e^{\frac{1}{4}\gamma\alpha^2} \tag{25}$$

$$\int_{\mathbb{R}} x\cosh[x\alpha]e^{-\frac{(x-\mu)^2}{\gamma}}dx = \sqrt{\pi\gamma}\left[\frac{\alpha\gamma}{2}\sinh(\mu\alpha) + \mu\cosh(\mu\alpha)\right]e^{\frac{1}{4}\gamma\alpha^2} \tag{26}$$

$$\int_{\mathbb{R}} x\sinh[x\alpha]e^{-\frac{(x-\mu)^2}{\gamma}}dx = \sqrt{\pi\gamma}\left[\frac{\alpha\gamma}{2}\cosh(\mu\alpha) + \mu\sinh(\mu\alpha)\right]e^{\frac{1}{4}\gamma\alpha^2} \tag{27}$$

From sections 9.24 and 9.25 of [22], we extract:

$$\mathcal{D}_{-B}(x) = \frac{e^{-\frac{x^2}{4}}}{\Gamma(B)}\int_{\mathbb{R}^+} e^{-x\zeta-\frac{\zeta^2}{2}}\zeta^{B-1}d\zeta, \quad (\mathcal{R}(B)>0) \quad \text{(see [22], 9.241/2)} \tag{28}$$

$$\begin{cases} \mathcal{Y}_B(x) := \frac{1}{2}\left[\mathcal{D}_{-B}(x) + \mathcal{D}_{-B}(-x)\right] = \sqrt{\frac{2}{\pi}}\frac{e^{-\frac{x^2}{4}}}{\Gamma(B)}\int_{\mathbb{R}^+}\cosh(x\,\zeta)e^{-\frac{\zeta^2}{2}}\zeta^{B-1}\,d\zeta, \\ \frac{d^2}{dx^2}\left\{\mathcal{Y}_B(x)\right\} = \left[\frac{x^2}{4} + \left(B - \frac{1}{2}\right)\right]\mathcal{Y}_B(x), \quad (B \geq 0), \quad \text{(see [22], 9.255/1)} \end{cases} \tag{29}$$

5.2 Quadratures

Let us define the couple of quadratures:

$$\mathcal{J}_i(m,s,B) = \int_{\mathbb{R}} x^i \mathcal{Y}_B(x) e^{-\frac{(x-m)^2}{2s}}\,dx, \quad i = 0, 1. \tag{30}$$

0^{th}-order moment - $\boldsymbol{\mathcal{J}_0(m,B)}$ Using the integral representation given in Eq.(29), we can write:

$$\begin{aligned} \mathcal{J}_0(m,s,B) &= \int_{\mathbb{R}}\left\{\mathcal{Y}_B(x)e^{-\frac{(x-m)^2}{2s}}\right\}dx \\ &= \sqrt{\frac{2}{\pi}}\frac{1}{\Gamma(B)}\int_{\mathbb{R}^+}\zeta^{[B-1]}e^{-\frac{\zeta^2}{2}}\left\{\int_{\mathbb{R}}\cosh(\zeta x)e^{-\frac{(x-m)^2}{2s}-\frac{x^2}{4}}dx\right\}d\zeta \end{aligned}$$

$$\mathcal{J}_0(m,s,B) = \sqrt{\frac{2}{\pi}}\frac{e^{-\frac{m^2}{2(2+s)}}}{\Gamma(B)}\int_{\mathbb{R}^+}\zeta^{[B-1]}e^{-\frac{\zeta^2}{2}}\left\{\int_{\mathbb{R}}\cosh(\zeta x)e^{-\frac{(2+s)}{4s}\left(x-\frac{2m}{2+s}\right)^2}dx\right\}d\zeta$$

Now we use Eq.(25) with $\gamma = 4s/(2+s)$ and $\mu = 2m/(2+s)$ to get

$$\mathcal{J}_0(m,s,B) = 2\sqrt{\frac{2}{\pi}}\sqrt{\frac{\pi s}{(2+s)}}\frac{e^{-\frac{m^2}{2(2+s)}}}{\Gamma(B)}\int_{\mathbb{R}^+}\zeta^{[B-1]}e^{-\frac{\zeta^2}{2}\left[\frac{2-s}{2+s}\right]}\cosh\left[\frac{2m\zeta}{2+s}\right]d\zeta$$

Let us introduce the renormalization $\eta := \zeta\sqrt{\frac{2-s}{2+s}}$, which implies

$$\mathcal{J}_0(m,s,B) = \sqrt{\frac{2}{\pi}}2\sqrt{\frac{\pi s}{2+s}}\frac{e^{-\frac{m^2}{2(2+s)}}}{\Gamma(B)}\left[\sqrt{\frac{2+s}{2-s}}\right]^B\underbrace{e^{+\frac{m^2}{(4-s^2)}}e^{-\frac{m^2}{(4-s^2)}}}_{=1}\int_{\mathbb{R}^+}\eta^{[B-1]}\cosh\left[\frac{2m\,\eta}{\sqrt{4-s^2}}\right]e^{-\frac{\eta^2}{2}}\,d\eta. \tag{31}$$

Finally, using the definition Eq.(29), we end up with:

$$\mathcal{J}_0(m,s,B) = 2\sqrt{\frac{\pi s}{2+s}}\left[\sqrt{\frac{2+s}{2-s}}\right]^B e^{\frac{m^2 s}{2(4-s^2)}}\mathcal{Y}_B\left(\frac{2m}{\sqrt{4-s^2}}\right). \tag{32}$$

First order moment - $\boldsymbol{\mathcal{J}_1(m,s,B)}$ From the definitions Eqs.(28) and (30), we observe that one can write:

$$\mathcal{J}_1(m,s,B) := \int_{\mathbb{R}}\left\{x\,\mathcal{Y}_B(x)e^{-\frac{(x-m)^2}{2s}}\right\}dx$$

From the previous equation and the definition of $\mathcal{J}_0(m,s,B)$ given in Eq.(30), let us observe that we can write:

$$\frac{d}{dm}\mathcal{J}_0(m,s,B) = \int_{\mathbb{R}}\left\{\left[\frac{(x-m)}{s}\right]\mathcal{Y}_B(x)e^{-\frac{(x-m)^2}{2s}}\right\}dx = \frac{1}{s}\mathcal{J}_1(m,s,B) - \frac{m}{s}\mathcal{J}_0(m,s,B).$$

This is equivalent to the relation:

$$\mathcal{J}_1(m,s,B) = m\mathcal{J}_0(m,s,B) + s\left[\frac{d}{dm}\mathcal{J}_0(m,s,B)\right]. \tag{33}$$

Using Eqs.(32) and (33), the conditioned expectation reads:

$$\mathbb{E}(x|\mathcal{Z}_t) = \left.\frac{\mathcal{J}_1(m.b,B)}{\mathcal{J}_0(m,s,B)}\right|_t = m + s\left[\frac{d}{dm}\left(\log\left\{\mathcal{J}_0(m,s,B)\right\}\right)\right]\Big|_t = \frac{4}{4-s^2}m(z) + \frac{2s}{\sqrt{4-s^2}}f_B\left(\frac{2\,m(z)}{\sqrt{4-s^2}}\right) \tag{34}$$